THE UNIVERSITY of EDINBURGH

Edinburgh Research Explorer

Coexistence and criticality of fluids with long-range potentials

Citation for published version:
Camp, PJ & Patey, GN 2001, 'Coexistence and criticality of fluids with long-range potentials', *The Journal of Chemical Physics*, vol. 114, no. 1, pp. 399-408. https://doi.org/10.1063/1.1329134

Digital Object Identifier (DOI):
10.1063/1.1329134

Link:
Link to publication record in Edinburgh Research Explorer

Document Version:
Publisher's PDF, also known as Version of record

Published In:
The Journal of Chemical Physics

Publisher Rights Statement:
Copyright 2001 American Institute of Physics. This article may be downloaded for personal use only. Any other use requires prior permission of the author and the American Institute of Physics.

General rights
Copyright for the publications made accessible via the Edinburgh Research Explorer is retained by the author(s) and / or other copyright owners and it is a condition of accessing these publications that users recognise and abide by the legal requirements associated with these rights.

Take down policy
The University of Edinburgh has made every reasonable effort to ensure that Edinburgh Research Explorer content complies with UK legislation. If you believe that the public display of this file breaches copyright please contact openaccess@ed.ac.uk providing details, and we will remove access to the work immediately and investigate your claim.

OPEN ACCESS

Download date: 06. May. 2023

Coexistence and criticality of fluids with long-range potentials

Philip J. Camp and G. N. Patey

Citation: J. Chem. Phys. **114**, 399 (2001); doi: 10.1063/1.1329134
View online: http://dx.doi.org/10.1063/1.1329134
View Table of Contents: http://jcp.aip.org/resource/1/JCPSA6/v114/i1
Published by the AIP Publishing LLC.

Additional information on J. Chem. Phys.

Journal Homepage: http://jcp.aip.org/
Journal Information: http://jcp.aip.org/about/about_the_journal
Top downloads: http://jcp.aip.org/features/most_downloaded
Information for Authors: http://jcp.aip.org/authors

ADVERTISEMENT

Downloaded 09 Aug 2013 to 129.215.221.120. This article is copyrighted as indicated in the abstract. Reuse of AIP content is subject to the terms at: http://jcp.aip.org/about/rights_and_permissions

Coexistence and criticality of fluids with long-range potentials

Philip J. Camp
Department of Chemistry, University of British Columbia, Vancouver, British Columbia V6T 1Z1, Canada and Department of Chemistry, University of Edinburgh, West Mains Road, Edinburgh EH9 3JJ, United Kingdom

G. N. Patey
Department of Chemistry, University of British Columbia, Vancouver, British Columbia V6T 1Z1, Canada

(Received 15 September 2000; accepted 5 October 2000)

Using mixed-field finite-size scaling simulations, we have investigated the liquid–vapor critical behavior of three-dimensional fluids with algebraically decaying attractive pair interactions, which vary like $-1/r^{3+\sigma}$ with $\sigma=3$, 1, and 0.1. The finite-size scaling analysis was carried out by matching the critical ordering operator distribution, $p_L(x)$, against the limiting Ising form, i.e., Ising criticality was assumed. When the potential is short-ranged ($\sigma=3$) the simulation results are entirely consistent with the expected Ising critical behavior. When the potential is long-ranged ($\sigma=1$, 0.1), however, marked deviations from Ising behavior are observed, particularly in the form of the critical ordering operator distribution, and in the estimated values of β/ν. The results are consistent with non-Ising criticality which is predicted theoretically in fluids with long-range interactions. Some results from Gibbs ensemble simulations are also provided in order to sketch the shape of the liquid–vapor coexistence envelope. We discuss the relevance of our results to the current issue of criticality in ionic fluids. © *2001 American Institute of Physics.*
[DOI: 10.1063/1.1329134]

I. INTRODUCTION

The criticality of phase separation in ionic fluids has received a great deal of attention recently. In experiments, Ising-like criticality,[1] classical criticality,[2,3] and a crossover between classical and Ising-like regimes[4] have been observed in a variety of systems. From simulation studies of the restricted primitive model (RPM) of ionic solutions[5] it is known that there is a high degree of ion association in the vicinity of the critical point. Therefore, the ionic fluid might be best considered as a mixture of dipolar ion pairs and a small concentration of free ions.[6] In this case, the predominant interactions are those between ion pairs, which vary like $1/r^3$, and those between free ions and ion pairs, which vary like $1/r^2$, bearing in mind that all of these interactions would be screened at least over very large distances by the low concentration of free ions. Although there are many three-dimensional fluids with prominent dipole–dipole interactions, positional and orientational averaging produces an asymptotic attractive ''effective pair interaction'' that varies like $-1/r^6$ for which the usual Ising criticality is expected.[7] In the case of ionic fluids, positional and orientational averaging similarly produces an asymptotic attractive interaction that varies like $-1/r^4$. This is a ''long-range'' interaction (defined below) that may be a source of non-Ising criticality. The consensus amongst previous simulation studies of RPM criticality is that the phase separation is Ising-like,[8–10] although it is unclear how non-Ising critical behavior would manifest itself in finite-size simulation results. It is therefore of interest to explore the effects of long-range interactions on fluid criticality, and how they become apparent in simulation results.

Amongst the earliest theoretical investigations of the effect of long-range attractive interactions on the critical behavior of one-component fluids was that by Stell,[11] who analyzed the behavior of near-critical correlations using the Ornstein–Zernike equation. On the assumption of homogeneity of the direct correlation function, it was found that if the range of the potential was sufficiently large, then one should expect exponents which deviate from the usual Ising exponents.[12,13] Subsequent work by Fisher *et al.*,[14] and by Sak,[15] largely involved renormalization group calculations on lattice models with algebraically decaying interactions. In all of these studies the pair potential under consideration had the asymptotic form $v(r)\sim -1/r^{D+\sigma}$ as $r\to\infty$, where D is the dimensionality, and the range parameter $\sigma>0$ for the thermodynamic limit to exist. On the basis of the work by Stell,[11–13] Fisher *et al.*,[14] and Sak,[15] three regimes of critical behavior are predicted, strictly for $D<4$: (i) with $\sigma\geqslant 2-\eta_{\mathrm{SR}}$ the potential is short-ranged and the exponents should assume the usual Ising values; η_{SR} is the Ising value of the correlation decay exponent, equal to 0.0335 ± 0.0025 in three dimensions;[16] (ii) with $D/2<\sigma<2-\eta_{\mathrm{SR}}$, the exponents should be functions of σ that interpolate between the Ising and classical values; (iii) with $\sigma<D/2$ the exponents should be equal to the classical (mean-field) values. The critical behavior in the latter regime has been rigorously determined for a ferromagnetic Ising model with algebraically decaying interactions by Aizenman and Fernández.[17] From these considerations we shall take ''long-range interactions'' to mean those for which $v(r)\sim -1/r^{D+\sigma}$ as $r\to\infty$, with $\sigma<2-\eta_{\mathrm{SR}}$.

Recently, Luijten and Blöte[18] performed extensive finite-size scaling computer simulations to confirm the existence of

 © 2001 American Institute of Physics

Downloaded 09 Aug 2013 to 129.215.221.120. This article is copyrighted as indicated in the abstract. Reuse of AIP content is subject to the terms at: http://jcp.aip.org/about/rights_and_permissions

classical critical behavior in ferromagnetic Ising models with algebraically decaying interactions in $D=1,2,3$, with $\sigma < D/2$. Their analysis involved measuring the cumulant ratio $Q(T,L)=\langle M^2\rangle_{T,L}^2/\langle M^4\rangle_{T,L}$, where M is the spontaneous magnetization, as a function of lattice size, L, and temperature, T, in the vicinity of the critical point. $Q(T,L)$ can be expanded as a universal constant, Q_0, plus terms involving L and T with exponents that characterize the universality class to which the critical behavior belongs.[18,19] After fitting this form to the simulation data, the exponents and Q_0 so obtained were in excellent agreement with the predicted classical values. The range $D/2<\sigma<2-\eta_{\mathrm{SR}}$ remains untested, however.

Real fluids lack the trivial up-down symmetry of the ferromagnetic Ising Hamiltonian, and this requires that the parameter analogous to the magnetization is not just the order parameter (the number density). Rehr and Mermin[20] have given a modification of Widom's original scaling hypothesis[21] for the equation of state in the region of the liquid-vapor critical point. If the coexistence chemical potential is an analytic function of temperature at the critical point, which is true for some solvable asymmetric models,[22–24] then the analog of the magnetization is an ordering operator, $\mathcal{M}\propto\rho-su$, where ρ is the number density, u is the energy density, and s is a nonuniversal mixing parameter (s is connected with the presence of a singularity in the coexistence diameter at the critical point). Bruce and Wilding[25,26] have exploited field-mixing to locate the critical points of simple fluids by comparing the distribution of $\mathcal{M}$ measured in a finite-size simulation, with the distribution of M in the Ising model at its critical point. To be clear, the form of the ordering operator distribution function, $p(x)$, is expected to be characteristic of the universality class to which the critical behavior belongs. The distributions appropriate to two- and three-dimensional short-range potentials, $p_{\mathrm{Is}}^{\star}(x)$, have been measured in large-scale computer simulations of the corresponding two-dimensional[27] and three-dimensional[28] Ising models. The apparent critical parameters of the fluid, $\mu_c(L)$ and $T_c(L)$, are those at which $p_L(x)$ collapses onto the universal form, $p_{\mathrm{Is}}^{\star}(x)$. The infinite-volume critical parameters are then estimated by extrapolating the values measured for several different system sizes to the limit $L^{-1}\to 0$. Since most simple fluids are expected to belong to the Ising universality class, this has been assumed in all published studies of three-dimensional fluid criticality. In principle this method could also be used to locate the critical points of fluids that belong to any known universality class, provided the corresponding critical distribution of the ordering operator is known *a priori*.

With regard to the identification of $\mathcal{M}$, it is commonly assumed that the coexistence chemical potential in real fluids is an analytic function of temperature. Recently, however, Fisher and Orkoulas[29,30] have analyzed previously published experimental data for propane, and carbon dioxide, which suggest that $(\partial^2\mu/\partial T^2)$ along the critical isochore *diverges* at the critical point, i.e., the coexistence chemical potential is not analytic at the critical point. This possibility was considered by Rehr and Mermin,[20] and for the particular case of a diverging second derivative they state that, ''the scaling equation would be rather uncomfortable to work with.'' Fisher and Orkoulas suggest that terms involving the pressure should appear in the prescription of $\mathcal{M}$,[29,30] but as yet no concrete conclusions have been put forward.

This problem notwithstanding, we have carried out a simulation study of vapor–liquid coexistence and criticality in three-dimensional fluids with long-range potentials. One of the motivations for this work is to investigate whether the effects of long-range interactions can be detected in finite-size simulations, which would clearly be of relevance to situations where the criticality is, as yet, uncertain, e.g., in ionic fluids. We have explored the criticality of a fluid of hard spheres interacting via an algebraically decaying attractive tail. The model pair potential we consider, $v(r)$, is defined by

$$v(r)=\begin{cases}\infty & r<d\\ -\epsilon(d/r)^{3+\sigma} & r\geqslant d\end{cases}, \tag{1}$$

where r is the pair separation, d is the hard-sphere diameter, ϵ is the well-depth, and σ is the interaction range parameter. We have investigated the long-range potentials with $\sigma=0.1$ and $\sigma=1$, for which classical critical behavior is predicted. For comparison, we have also studied the case $\sigma=3$ which is expected to exhibit the usual $D=3$ Ising critical behavior. We have utilized the grand canonical finite-size scaling method proposed by Bruce and Wilding[25,26] (including the original definition of $\mathcal{M}$) to analyze extensive simulation results. Unfortunately, the mean-field critical ordering operator distribution, $p_{\mathrm{cl}}^{\star}(x)$, is not yet known with any confidence, but there is one approximate analytical expression for $p_{\mathrm{cl}}^{\star}(x)$ given by Hilfer[31] which depends solely on the equation-of-state exponent, δ; $\delta=3$ for mean-field critical points, and $\delta=4.8$ for $D=3$ Ising critical points.[32] We have therefore carried out much of the mixed-field finite-size scaling analysis assuming Ising criticality. We will, however, assess the consistency of the results with Ising critical behavior by extracting the exponent ratio β/ν from the finite-size scaling analysis, and also by comparing the measured ordering operator distributions with the Ising form. We shall show that there are marked inconsistencies in the results for $\sigma=0.1$ and $\sigma=1$. In particular we shall show that the apparent critical ordering operator distributions for the long-range potentials cannot be well matched with the limiting Ising form, and that the measured exponent ratio β/ν disagrees with the accepted Ising value. It shall also be noted that in the long-range systems $p_L(x)$ does not agree with Hilfer's form for $p_{\mathrm{cl}}^{\star}(x)$ either; this may not be particularly significant, however, due to the approximate nature of the theoretical universal distribution. For comparison, we show that the results for $\sigma=3$ are in excellent agreement with the expected Ising behavior.

To obtain *rough estimates* of the critical parameters for each potential, we assume Ising forms and make the best possible fits of $p_L(x)$ to $p_{\mathrm{Is}}^{\star}(x)$. The critical parameters so obtained are then used to test a relation, due to Brilliantov and Valleau,[33] which links the range of the potential with the critical temperature and density arising from the Gaussian approximation (see, e.g., Ref. 34). We shall show that this mean-field relation becomes more reliable as the range of the

Downloaded 09 Aug 2013 to 129.215.221.120. This article is copyrighted as indicated in the abstract. Reuse of AIP content is subject to the terms at: http://jcp.aip.org/about/rights_and_permissions

TABLE I. Critical parameters determined from mixed-field finite-size scaling, using the method of Bruce and Wilding assuming Ising criticality (see text). T_c^* is the reduced critical temperature, ρ_c^* is the reduced critical density, u_c^* is the reduced critical configurational energy density, μ_c^* is the reduced critical chemical potential, and s is the mixing parameter.

Model	T_c^*	ρ_c^*	u_c^*	μ_c^*	β/ν	s
$\sigma=3$	0.5972(1)	0.3757(4)	−0.548(2)	−2.577(1)	0.54(1)	−0.04
$\sigma=1$	1.3724(1)	0.2993(1)	−0.6594(7)	−2.6143(2)	0.80(5)	−0.03
$\sigma=0.1$	11.452(8)	0.247(5)	−3.8(2)	−2.791(1)	0.82(4)	−0.006
$D=3$ Ising[a]					0.518(7)	
Classical					1	

[a]Reference 32.

potential increases, which suggests that classical criticality is being approached. Finally, for each potential we also provide some results from Gibbs ensemble Monte Carlo simulations,[35,36] in order to sketch the subcritical portions of the vapor–liquid coexistence curves.

This paper is organized as follows. We shall begin by summarizing the finite-size scaling analysis in Sec. II. In Sec. III we give details of the grand canonical and Gibbs ensemble Monte Carlo simulations. The results are presented in Sec. IV, and a discussion in Sec. V concludes the paper.

II. FINITE-SIZE SCALING

For reference, we shall summarize the various relations and scaling laws which are used in the simulation of critical points.[37] In mixed-field finite-size scaling, an ordering operator, $\mathcal{M}$, is identified as being analogous to the magnetization in the Ising model,

$$\mathcal{M}\propto\rho-su. \tag{2}$$

In order to compare the distribution of $\mathcal{M}$ at the critical point with a universal limiting form, a variable, x, is defined by,

$$x=(\mathcal{M}-\langle\mathcal{M}\rangle_L)/\delta\mathcal{M}_L, \tag{3}$$

where $\langle\cdots\rangle_L$ denotes an expectation value in a finite-size system with dimension L, and $\delta\mathcal{M}_L$ is the standard deviation. With this definition, the normalized probability distribution, $p_L(x)$, has zero mean and unit variance. The standard deviation measured in a finite-size system follows the asymptotic scaling law,

$$\delta\mathcal{M}_L=a_{\mathcal{M}}L^{-\beta/\nu}, \tag{4}$$

where $a_{\mathcal{M}}$ is a nonuniversal constant, and β and ν are the order parameter and correlation length exponents, respectively. For the $D=3$ Ising model, $\beta=0.326(4)$, $\nu=0.6294(2)$, and $\beta/\nu=0.518(7)$.[32] The Ising and classical values of β/ν are also recorded in Table I. In Bruce and Wilding's method, the apparent finite-size critical parameters are those for which $p_L(x)$ collapses onto the appropriate universal limiting form, which must be known *a priori*. The finite-size critical temperature and chemical potential then scale like,

$$T_c(L)-T_c(\infty)\propto L^{-(\theta+1)/\nu}, \tag{5}$$

$$\mu_c(L)-\mu_c(\infty)\propto L^{-(\theta+1)/\nu}, \tag{6}$$

where $T_c(\infty)$ and $\mu_c(\infty)$ are the infinite-volume critical parameters, and θ is the Wegner[38] correction-to-scaling exponent. For $D=3$ Ising criticality, Chen *et al.*[39] estimate $\theta\simeq0.54(5)$. Ignoring corrections to scaling, the finite-size number density and energy density scale like

$$\rho_c(L)-\rho_c(\infty)\propto L^{-(1-\alpha)/\nu}, \tag{7}$$

$$u_c(L)-u_c(\infty)\propto L^{-(1-\alpha)/\nu}, \tag{8}$$

where α is the specific-heat exponent. For nonclassical critical points, the hyperscaling relation $2-\alpha=D\nu$ implies that the number density and energy density scale with $L^{-(D-1/\nu)}$, which is the scaling law we shall use where Ising criticality is assumed.

Another method of extracting critical parameters and exponents is to measure the moment ratio $Q(K,L)=\langle\mathcal{M}^2\rangle_{K,L}^2/\langle\mathcal{M}^4\rangle_{K,L}$, where $K=1/k_BT$, for many temperatures and system sizes, and fit the results to an appropriate expansion. For Ising critical points a Taylor expansion in $K-K_c$ and L yields[19]

$$Q(K,L)=Q_0+a_1(K-K_c)L^{y_t}+a_2(K-K_c)^2L^{2y_t}+a_3(K-K_c)^3L^{3y_t}+\cdots+b_1L^{y_i}+\cdots, \tag{9}$$

where Q_0, y_t, and y_i are universal. The corresponding equation for classical critical points was given in Ref. 18 as

$$Q(T,L)=Q_0^*+p_1(T-T_c)L^{y_t^*}+p_2(T-T_c)^2L^{2y_t^*}+p_3(T-T_c)^3L^{3y_t^*}+\cdots+q_1L^{-D/2}+q_2L^{y_i^*/2}+q_3L^{y_i^*}+\cdots. \tag{10}$$

The universal Ising and classical values in Eqs. (9) and (10), respectively, are given in Table II. The drawback of this

TABLE II. Critical parameters determined from mixed-field finite-size scaling, using the moment ratio method (see text). T_c^* is the reduced critical temperature, Q_0 and y_t are the universal Ising exponents appearing in Eq. (9), and Q_0^* and y_t^* are the universal classical exponents appearing in Eq. (10).

Model	T_c^*	Q_0	y_t	Q_0^*	y_t^*
$\sigma=3$	0.5972(3)	0.64(2)	1.64(5)		
$D=3$ Ising[a]		0.623	1.538		
Classical[b]				0.457	1

[a]Reference 19.
[b]Reference 45.

Downloaded 09 Aug 2013 to 129.215.221.120. This article is copyrighted as indicated in the abstract. Reuse of AIP content is subject to the terms at: http://jcp.aip.org/about/rights_and_permissions

method is that the two-dimensional fits involve many free parameters, and so it can prove difficult to obtain satisfactory results.

III. COMPUTER SIMULATIONS

In the following it will be useful to define various reduced quantities in terms of the interaction parameters, the temperature, T, the volume, V, and Boltzmann's constant, k_B: the reduced temperature, $T^*=k_BT/\epsilon$; the reduced reciprocal temperature, $K^*=1/T^*$; the reduced number density, $\rho^*=\rho d^3$, where $\rho=N/V$ and N is the number of particles; the reduced configurational energy, $U^*=U/\epsilon$; the reduced configurational energy density, $u^*=ud^3/\epsilon$, where $u=U/V$; the reduced chemical potential, $\mu^*=\mu/k_BT-3\ln(\Lambda/d)$, where μ is the chemical potential, and Λ is the de Broglie thermal wavelength.

All of the simulations were performed with cubic simulation cells of side L, and with periodic boundary conditions applied. In all of the simulations the pair potential was truncated at a distance $r_{\rm cut}=L/2$. This choice of $r_{\rm cut}$ is necessary for the finite-size scaling calculations, since in the limit $L\to\infty$ the energy must correspond to that for the full potential in Eq. (1). The long-range contribution, $U_{\rm LR}$, was calculated by assuming that the pair-correlation function $g(r)=1$ for $r\geqslant r_{\rm cut}$, in the usual way,[40]

$$U_{\rm LR}=2\pi N\rho\int_{r_{\rm cut}}^{\infty}r^2g(r)v(r)\mathrm{d}r\simeq-\frac{2\pi N\rho^*\epsilon}{\sigma}\cdot\left(\frac{d}{r_{\rm cut}}\right)^{\sigma}. \quad (11)$$

A. Gibbs Ensemble Monte Carlo simulations

To sketch out the vapor–liquid coexistence curves for each of the systems, Gibbs Ensemble Monte Carlo (GEMC) simulations[35,36] were performed with a total of $N=512$ particles. One MC sweep consisted of, on average, an attempted translation of each particle, one attempted volume transfer, and N attempted particle transfers. The maximum translational displacement in each box, and the maximum volume change were adjusted to give a 50% acceptance rate. Each simulation was started with random configurations at the same density for each subsystem. The total volume of the subsystems was chosen so that, on average, approximately 100 particles were in the vapor phase. In every case the run consisted of 10^5 MC sweeps for equilibration, followed by a production run of 9×10^5 MC sweeps. Averages of thermodynamic quantities were accumulated over blocks of 10^3 MC sweeps. Statistical errors were estimated by assuming that the block averages were uncorrelated. The chemical potentials in the two coexisting phases were estimated using the expression due to Smit and Frenkel.[41]

B. Grand Canonical Monte Carlo simulations

For the investigation of the critical points, Grand Canonical Monte Carlo (GCMC) simulations[40] were performed with box sizes in the range $L/d=9-15$. For $\sigma=0.1$ we also carried out simulations with $L/d=17$. One MC sweep consisted of about $2\langle N\rangle$ insertion/deletion attempts, where $\langle N\rangle$ is the average number of particles in the box—this leads to similar statistical accuracy for each of the box sizes simulated. No particle translations were attempted, rather, the sampling of configuration space was achieved solely by the insertion and deletion of particles.

For each potential and system size, the joint probability distribution $p_L(\rho,u)$ was calculated during a preliminary run close to where the critical point was indicated by the GEMC simulations. Using standard histogram reweighting techniques,[42] we determined, by inspection, the temperature, chemical potential, and mixing parameter, s, for which the distribution $p_L(x)$ most closely matched the limiting Ising form, $p^\star_{\rm Is}(x)$. Using these parameters, a much longer run was used to generate $p_L(\rho,u)$, from which the final estimates for $T_c^*(L)$, $\mu_c^*(L)$, and s were fine tuned. For each potential and system size, the final run consisted of 10^7 MC sweeps.

IV. RESULTS

A. $\sigma=3$

To check the accuracy of our mixed-field finite-size scaling analysis, and to provide a benchmark for the results for long-range potentials, we have performed calculations on the system with $\sigma=3$, for which the criticality is expected to belong to the Ising universality class. The results of GEMC calculations are reported in Table III. In Fig. 1 we show a portion of the vapor-liquid coexistence curve as determined by GEMC simulations, along with the line $\rho^*=\frac{1}{2}(\rho^*_{\rm vapor}+\rho^*_{\rm liquid})$; clearly the coexistence diameter singularity cannot be resolved in the simulation results. Also shown is the critical point determined by the Bruce and Wilding method, as follows.

In Fig. 2 the critical ordering operator distribution, $p_L(x)$, is shown for the two largest system sizes, $L/d=13$ and $L/d=15$, along with the universal distribution, $p^\star_{\rm Is}(x)$, reported in Ref. 28. The simulation curves in Fig. 2 were symmetrized with a mixing parameter $s=-0.04$. It is clear that the finite-size distributions collapse almost perfectly onto the universal form. A similar level of agreement was found for the smaller systems as well.

In Fig. 3 we show the standard deviation, $\delta\mathcal{M}_L$, as a function of $L^{-\beta/\nu}$, with $\beta/\nu=0.518(7)$ being the established Ising value.[32] The plot is linear for the three largest system sizes, and an extrapolation of these results to $L^{-1}\to0$ appears to intercept the ordinate at the origin, in accordance with Eq. (4). In fact, a fit of the results for the three largest system sizes to Eq. (4) yields the exponent ratio $\beta/\nu=0.54(1)$, which is in good agreement with the established Ising value, taking into account the uncertainties.

In Fig. 4 we show the apparent finite-size critical temperatures and densities. $T_c^*(L)$, $\mu_c^*(L)$, $\rho_c^*(L)$, and $u_c^*(L)$ for the three largest system sizes were fitted to Eqs. (5)–(8) with the Ising exponents to yield estimates of the infinite-volume critical parameters given in Table I. The resulting critical point in the ρ^*-T^* plane is shown in Fig. 1.

Also shown in Fig. 1 is a fit of the liquid-phase coexistence density (ρ_+^*) and the vapor-phase coexistence density (ρ_-^*) to the form,

$$\rho_\pm^*-\rho_c^*=A|T^*-T_c^*|\pm B|T^*-T_c^*|^{\beta'}. \quad (12)$$

Downloaded 09 Aug 2013 to 129.215.221.120. This article is copyrighted as indicated in the abstract. Reuse of AIP content is subject to the terms at: http://jcp.aip.org/about/rights_and_permissions

TABLE III. Properties of coexisting vapor and liquid phases as a function of reduced temperature, T^*, from GEMC simulations of $N=512$ particles: ρ^* is the reduced density, U^*/N is the reduced configurational energy per particle, and μ^* is the reduced chemical potential. The numbers in parentheses denote the statistical uncertainty in the last digit.

	Vapor phase			Liquid phase		
T^*	ρ^*	U^*/N	μ^*	ρ^*	U^*/N	μ^*
			$\sigma=3$			
0.50	0.034(4)	−0.09(3)	−3.49(6)	0.83(1)	−3.12(6)	−3.4(4)
0.52	0.056(6)	−0.27(3)	−3.31(6)	0.78(1)	−2.89(6)	−3.3(2)
0.54	0.08(1)	−0.36(6)	−3.08(7)	0.73(1)	−2.67(8)	−3.1(1)
0.56	0.11(1)	−0.47(5)	−2.90(3)	0.67(1)	−2.41(6)	−2.90(9)
0.58	0.16(2)	−0.66(7)	−2.72(3)	0.59(2)	−2.10(8)	−2.72(6)
			$\sigma=1$			
1.10	0.034(3)	−0.21(2)	−3.49(7)	0.69(1)	−5.3(1)	−3.49(8)
1.15	0.047(7)	−0.33(5)	−3.33(8)	0.64(2)	−4.9(2)	−3.33(8)
1.20	0.07(1)	−0.49(8)	−3.13(6)	0.60(2)	−4.5(2)	−3.13(6)
1.25	0.102(8)	−0.75(6)	−2.95(3)	0.55(1)	−4.2(1)	−2.95(3)
1.30	0.140(8)	−1.04(6)	−2.79(1)	0.500(9)	−3.72(8)	−2.79(2)
			$\sigma=0.1$			
8.50	0.021(1)	−1.3(1)	−4.0(1)	0.66(1)	−42(1)	−4.0(1)
9.00	0.029(2)	−1.8(1)	−3.69(6)	0.62(1)	−40(1)	−3.68(6)
9.50	0.041(3)	−2.6(2)	−3.44(5)	0.58(1)	−37(1)	−3.44(5)
10.00	0.055(5)	−3.5(3)	−3.25(4)	0.52(2)	−33(1)	−3.25(5)
10.50	0.084(9)	−5.3(6)	−3.07(4)	0.47(2)	−30(1)	−3.07(4)
10.75	0.12(1)	−7.6(7)	−2.97(2)	0.45(1)	−29(1)	−2.97(2)

Considering the range of temperatures included in the fit, and the finite-size of the simulation box, β' cannot be identified with the critical exponent β. Fitting the data to Eq. (12) yields the amplitudes $A=0.53$ and $B=0.91$, and the exponent $\beta'=0.36$. The value of the exponent is not too dissimilar from the Ising critical exponent, $\beta=0.326(4)$,[32] which shows that the critical scaling extends some way into the coexistence region. This was also observed in finite-size scaling simulations of the three-dimensional Lennard-Jones fluid in Ref. 37.

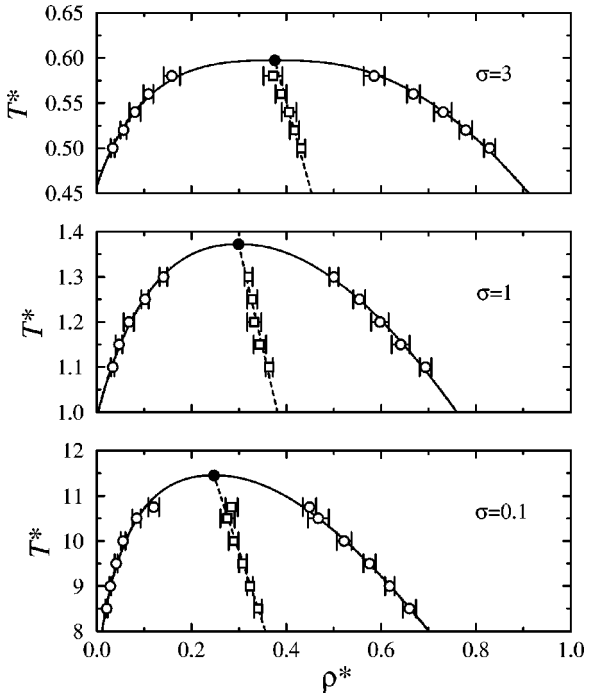

FIG. 1. Vapor–liquid coexistence curves in the density-temperature plane, for $\sigma=3$ (top), $\sigma=1$ (middle), and $\sigma=0.1$ (bottom): critical points estimated using the Bruce and Wilding method (solid circles); GEMC coexistence points (open circles); GEMC average densities (open squares); fit of coexistence curve to Eq. (12) (solid line); average density from fit (dotted line).

As an independent check of the critical parameters, we also analyzed the moment ratio, $Q(K,L)$, according to the Ising scaling form in Eq. (9). For each system size we used histogram reweighting to calculate $Q(K,L)$ at coexistence for several temperatures in the region of the critical point. Coexistence was determined by tuning the chemical potential, and s, until $p_L(x)$ was bimodal, with equal peak heights and peak areas. In Fig. 5 we show plots of $Q(K,L)$ against K^* for each system size. A fit to Eq. (9) was made with the value of y_i fixed at the Ising value -0.82. The most significant fit parameters, $T_c^*=1/K_c^*$, Q_0, and y_t are shown in

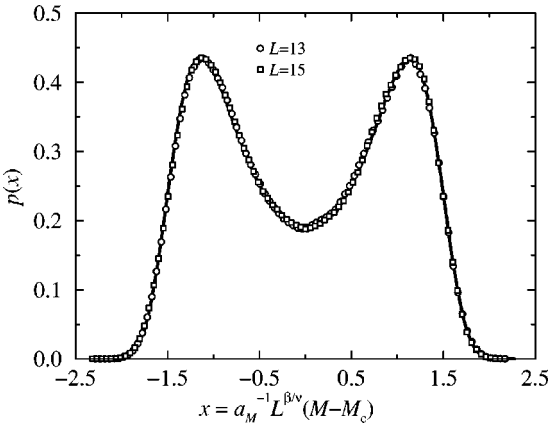

FIG. 2. Critical ordering operator distributions for $\sigma=3$: $p_L(x)$ for $L/d=13$ (circles) and $L/d=15$ (squares); limiting Ising distribution, $p_{\rm Is}^*(x)$, from Ref. 28 (solid line).

Downloaded 09 Aug 2013 to 129.215.221.120. This article is copyrighted as indicated in the abstract. Reuse of AIP content is subject to the terms at: http://jcp.aip.org/about/rights_and_permissions

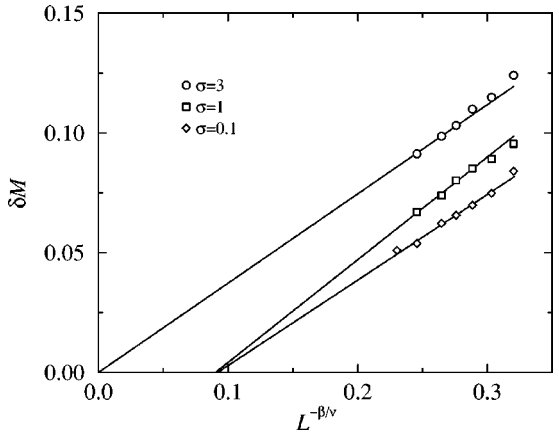

FIG. 3. Standard deviation, $\delta\mathcal{M}_L$, of the ordering operator, $\mathcal{M}$, as a function of $L^{-\beta/\nu}$, where L is the simulation box dimension, and β and ν are the order parameter and correlation decay exponents, respectively: $\sigma=3$ (circles); $\sigma=1$ (squares); $\sigma=0.1$ (diamonds). The lines are linear fits to the results for $L/d\geqslant 12$ in each case.

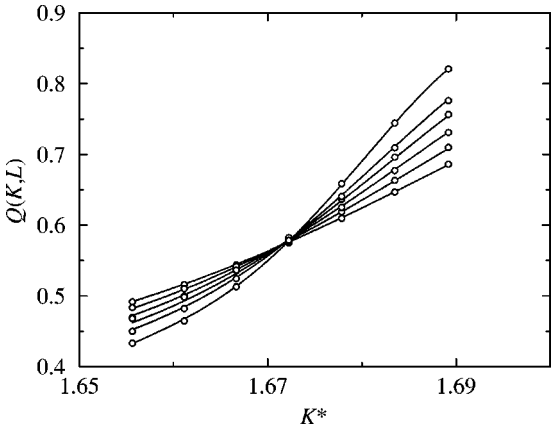

FIG. 5. Cumulant ratio, $Q(K,L)=\langle\mathcal{M}^2\rangle_{K,L}^2/\langle\mathcal{M}^4\rangle_{K,L}$, as a function of reduced temperature, K^*, for $\sigma=3$ and, from top right to bottom right, $L/d=15$, $L/d=13$, $L/d=12$, $L/d=11$, $L/d=10$, and $L/d=9$. The solid lines represent a fit to the simulation data using Eq. (9).

Table II. The critical temperature, T_c^*, is in excellent agreement with that obtained via the Bruce and Wilding method, and Q_0 and y_t are in good agreement with the established Ising values, also shown in the table.

Taken as a whole, the results of mixed-field finite-size scaling analysis for $\sigma=3$ are entirely consistent with the critical behavior belonging to the Ising universality class. Obviously, this is not a new result, but we stress that our simulations can provide convincing evidence of Ising universality. More importantly, these results provide a benchmark against which the results for long-range potentials can be assessed.

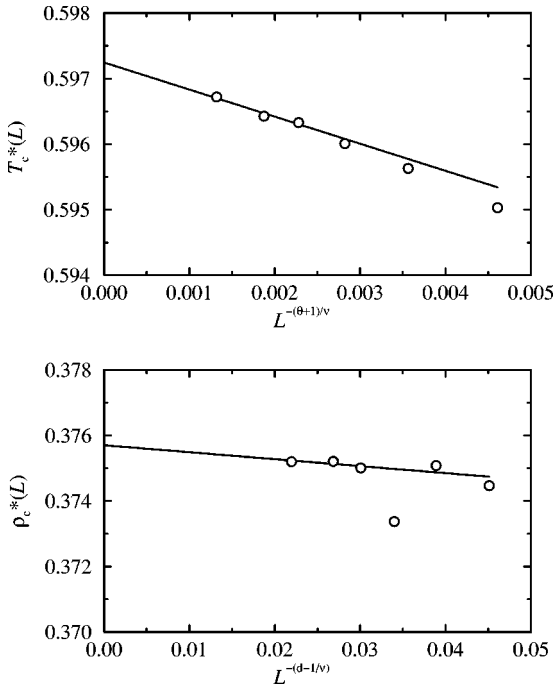

FIG. 4. Extrapolation of the critical temperature (top) and critical density (bottom) for $\sigma=3$ to the limit $L^{-1}\to 0$. The solid lines are extrapolations of the results for the three largest system sizes ($L/d\geqslant 12$).

B. $\sigma=1$

In Fig. 6 we show the apparent finite-size critical ordering operator distributions, $p_L(x)$, for $L/d=13$ and $L/d=15$, along with the assumed Ising limiting form, $p_{\mathrm{Is}}^{\star}(x)$. At first glance, $p_L(x)$ appears to collapse onto $p_{\mathrm{Is}}^{\star}(x)$ rather well. It proved impossible, however, to achieve as good a match as for $\sigma=3$ (compare with Fig. 2). We therefore had to choose some criteria for establishing the ''best'' estimates for the apparent critical parameters, $T_c^*(L)$ and $\mu_c^*(L)$. To this end, the matching was performed such that: (i) the distribution was symmetrical about $x=0$; (ii) the peak height matched that of the assumed Ising limiting form, $p_{\mathrm{Is}}^{\star}(x)$. The simulation curves in Fig. 6 were symmetrized with a mixing parameter $s=-0.03$. Figure 6 shows that the minimum at $x=0$ is too deep, and that the maxima occur at a value of $|x|$ which is too small. A similar discrepancy was found for all of the system sizes considered.

In Fig. 3 we show the standard deviation, $\delta\mathcal{M}_L$, as a function of $L^{-\beta/\nu}$, with $\beta/\nu=0.518(7)$ being the established Ising value.[32] A linear fit to the simulation results for the three largest system sizes intercepts the ordinate far from the

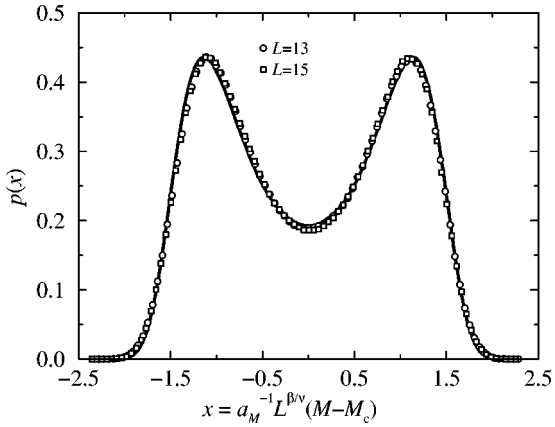

FIG. 6. Critical ordering operator distributions for $\sigma=1$: $p_L(x)$ for $L/d=13$ (circles) and $L/d=15$ (squares); limiting Ising distribution, $p_{\mathrm{Is}}^{\star}(x)$, from Ref. 28 (solid line).

Downloaded 09 Aug 2013 to 129.215.221.120. This article is copyrighted as indicated in the abstract. Reuse of AIP content is subject to the terms at: http://jcp.aip.org/about/rights_and_permissions

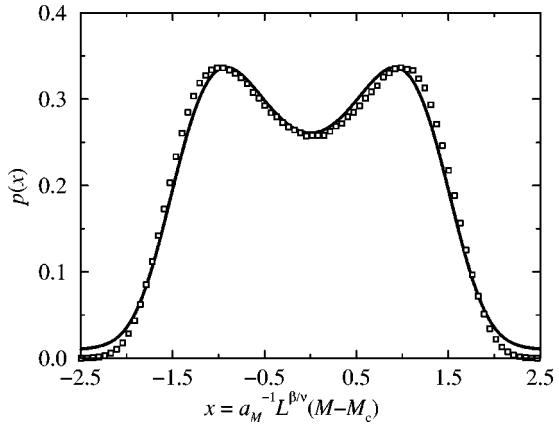

FIG. 7. Critical ordering operator distributions for $\sigma=1$: $p_L(x)$ for $L/d=15$ (squares); approximate classical distribution, $p_{\mathrm{cl}}^{\star}(x)$, from Ref. 31 (solid line).

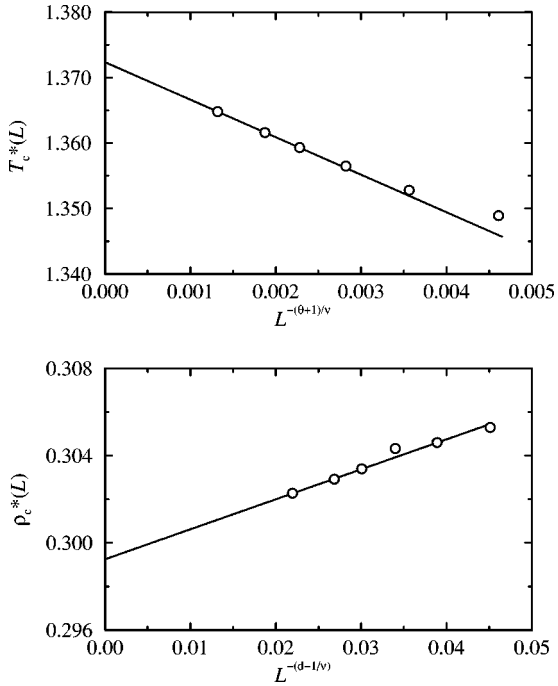

FIG. 8. Extrapolation of the critical temperature (top) and critical density (bottom) for $\sigma=1$ to the limit $L^{-1}\to 0$. The solid lines are extrapolations of the results for the three largest system sizes ($L/d\geqslant 12$).

origin, which constitutes a violation of the scaling law in Eq. (4). A fit of $\delta\mathcal{M}_L$ for the three largest system sizes to Eq. (4) yields the exponent ratio $\beta/\nu=0.80(5)$, which is very different from the Ising value.

It would appear, then, that the limiting critical ordering operator distribution for $\sigma=1$ does not correspond to the established Ising form, at least with the mixed-field ansatz expressed in Eq. (2). Unfortunately, the classical critical ordering operator distribution, $p_{\mathrm{cl}}^{\star}(x)$, has not yet been determined with any precision. Hilfer[31] has provided a prediction of this function, requiring only prior knowledge of the equation-of-state exponent. The integral of Hilfer's form does not converge, however, so to normalize the distribution requires an arbitrary cutoff in $|x|$. Nonetheless, when the distribution is cut off at $|x|=2.5$, Hilfer's form with $\delta=4.8$ is in fair agreement with simulation data for the $D=3$ Ising model.[28] In Fig. 7 we have attempted to match $p_L(x)$ for $L/d=15$ against Hilfer's estimate of $p_{\mathrm{cl}}^{\star}(x)$, with the same cutoff and $\delta=3$. The truncation is very prominent close to $|x|=2.5$, where the measured $p_L(x)$ has already become vanishingly small. Clearly, the simulation results cannot be matched onto the available estimate of the classical limiting form. This remains inconclusive, however, because of the approximate nature of the theoretical curve.

We have also attempted to carry out a finite-size analysis of the moment ratio, Q, but we were unable to achieve acceptable fits to either the Ising expansion in Eq. (9) *or* the classical expansion in Eq. (10). This is likely due to the large number of fit parameters, which are difficult to determine by fitting to a data set which only spans a limited range of system sizes. Although we were able to obtain satisfactory fits to the results with $\sigma=3$, it is quite possible that, using this method, larger system sizes are required for longer range potentials. This is currently beyond our computational ability.

Assuming the Ising limiting form, we can at least extract a rough estimate of the infinite-volume critical parameters. As for $\sigma=3$, we fitted the apparent finite-size critical parameters to Eqs. (5)–(8) with the Ising exponents, to yield the values shown in Table I. The fits to $T_c^*(L)$ and $\rho_c^*(L)$ are shown in Fig. 8. Coexistence results from GEMC simulations are reported in Table III, and shown in Fig. 1 along with our estimate of the critical point. The coexistence diameter was fitted to Eq. (12), with the amplitudes $A=0.22$ and $B=0.60$, and the exponent $\beta'=0.46$. The value of $\beta'=0.46$ is close to the mean-field value of $\beta=1/2$. This may not be significant, however, because the classical-to-Ising crossover, *if present*, occurs closer to the critical temperature as the range of the potential increases. Roughly speaking, classical-to-Ising crossover occurs when the density-density correlation length exceeds the range of the potential. Therefore, when the potential is long-ranged, one has to be closer to the critical point before the diverging density–density correlation length becomes comparable with the typical range of interaction.

C. $\sigma=0.1$

In Fig. 9 we show $p_L(x)$ for $\sigma=0.1$ and box sizes $L/d=13$, 15, and 17, along with $p_{\mathrm{Is}}^{\star}(x)$. The simulation curves in Fig. 9 were symmetrized with mixing parameter $s=-0.006$. It proved impossible to achieve an unambiguous collapse of $p_L(x)$ onto $p_{\mathrm{Is}}^{\star}(x)$, and so the matching was carried out as with $\sigma=1$, i.e., by matching peak heights. This procedure results in peaks which occur at a value of $|x|$ smaller than that at which the peaks in $p_{\mathrm{Is}}^{\star}(x)$ occur. Moreover, the minimum in $p_L(x)$ at $x=0$ is significantly deeper than that of $p_{\mathrm{Is}}^{\star}(x)$, with the discrepancy growing with increasing box size. This is a particularly significant observation because it suggests that a better match would not likely be achieved by simulating a larger system size, i.e., Ising criticality would not be observed, regardless of how large the system is.

Downloaded 09 Aug 2013 to 129.215.221.120. This article is copyrighted as indicated in the abstract. Reuse of AIP content is subject to the terms at: http://jcp.aip.org/about/rights_and_permissions

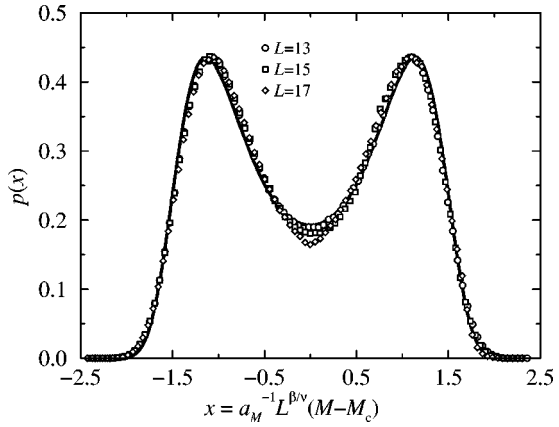

FIG. 9. Critical ordering operator distributions for $\sigma=0.1$: $p_L(x)$ for $L/d=13$ (circles), $L/d=15$ (squares), and $L/d=17$ (diamonds); limiting Ising distribution, $p^{\star}_{\rm cl}(x)$, from Ref. 28 (solid line).

In Fig. 3 we show $\delta\mathcal{M}_L$ against $L^{-\beta/\nu}$, with the Ising value of β/ν. As with $\sigma=1$, a linear fit to the results intercepts the ordinate far from the origin, which violates the scaling law in Eq. (4). A fit of $\delta\mathcal{M}_L$ for the four largest system sizes to Eq. (4) yields the exponent ratio $\beta/\nu=0.82(4)$. As for $\sigma=1$, the apparent value of β/ν is far from the Ising value.

We attempted to match $p_L(x)$ with Hilfer's estimate of $p^{\star}_{\rm cl}(x)$, but similar discrepancies were evident as with $\sigma=1$. We also tried to analyze the moment ratio, Q, using Eqs. (9) and (10), but it again proved impossible to obtain unambiguous fits.

To obtain at least rough estimates of the infinite-volume critical parameters for $\sigma=0.1$, we extrapolated the results for the four largest system sizes, using Eqs. (5)–(8) assuming Ising criticality. The resulting critical parameters are given in Table I, and the extrapolations of $T_c^*(L)$ and $\rho_c^*(L)$ are shown in Fig. 10. GEMC simulation results for the coexistence properties are reported in Table III, and the coexistence envelope is shown in Fig. 1. The coexistence diameter was fitted to Eq. (12), with the amplitudes $A=0.03$ and $B=0.20$, and the exponent $\beta'=0.46$. Once again, $\beta'=0.46$ is quite close to the classical value of $\beta=1/2$, but the same comments apply as for $\sigma=1$.

D. Comparison with the Gaussian approximation

Brilliantov and Valleau[33] have derived a mean-field relation between the critical temperature and the critical density for the liquid–vapor transition in fluids with hard cores and attractive tails. The pair potential is split into the hard-sphere potential, $v_{\rm HS}(r)$, plus an attractive perturbation, which in the Weeks–Chandler–Andersen (WCA) partition[43] remains finite in the hard-core region, i.e., $v(r)-v_{\rm HS}(r)=-\epsilon$ for $r\leqslant d$. The mean-field relation arises from the Gaussian approximation to the effective Hamiltonian obtained using the Hubbard–Schofield approach,[44] and it requires detailed knowledge of the reference hard-sphere fluid—see Ref. 33 for details. Using the Carnahan–Starling

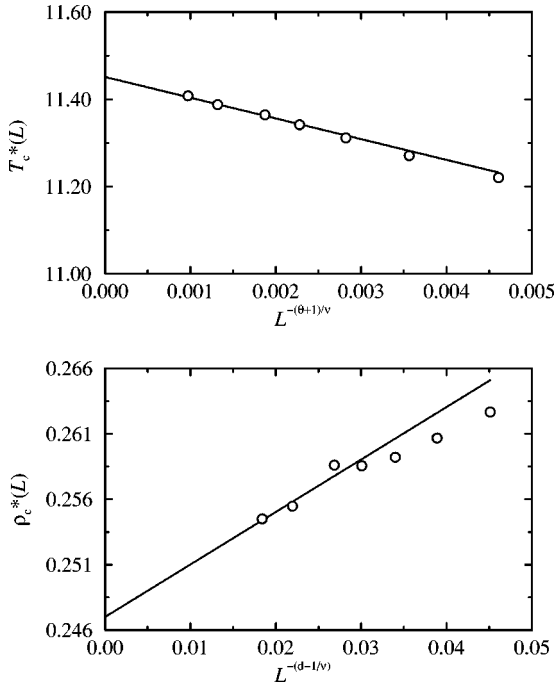

FIG. 10. Extrapolation of the critical temperature (top) and critical density (bottom) for $\sigma=0.1$ to the limit $L^{-1}\to 0$. The solid lines are extrapolations of the results for the four largest system sizes ($L/d\geqslant 12$).

expressions for the thermodynamics of the hard-sphere fluid, Brilliantov and Valleau showed that, within the Gaussian approximation,

$$\frac{k_BT_c}{\epsilon_{\rm eff}}=\frac{8\eta_c(1-\eta_c)^4}{1+4\eta_c+4\eta_c^2-4\eta_c^3+\eta_c^4}\equiv Z(\eta_c), \tag{13}$$

where $\eta_c=\pi\rho_c^*/6$ is the critical packing fraction, and $\epsilon_{\rm eff}$ is an effective well-depth given by

$$\epsilon_{\rm eff}=-\left(\frac{4\pi d^3}{3}\right)^{-1}\int d\mathbf{r}v(r). \tag{14}$$

With the WCA partition the effective well-depth for the attractive part of the potential studied in this work (1) is given by

$$\epsilon_{\rm eff}=\epsilon\left(1+\frac{3}{\sigma}\right). \tag{15}$$

Since Eq. (13) is a mean-field expression, it is expected to become more accurate as the range of the potential increases. Indeed, Brilliantov and Valleau have shown this to be the case using simulation estimates of the critical parameters in square-well fluids.[33]

We have tested Eq. (13) for the potentials studied in this work, bearing in mind that the rough estimates of the critical parameters reported in Table I were obtained assuming Ising expressions. In Table IV we present $(k_BT_c/\epsilon_{\rm eff})$, $Z(\eta_c)$, and the ratio of the two, as a function of σ. Clearly, Eq. (13) becomes more reliable as σ increases; the error for $\sigma=0.1$ is only about 2%. This is consistent with the general idea that classical criticality is approached as potential becomes longer ranged.

Downloaded 09 Aug 2013 to 129.215.221.120. This article is copyrighted as indicated in the abstract. Reuse of AIP content is subject to the terms at: http://jcp.aip.org/about/rights_and_permissions

TABLE IV. The critical parameter ratio, $Z(\eta_c)/(k_B T_c/\epsilon_{\text{eff}})$, as a function of the range parameter, σ. The various quantities are defined in Eqs. (13), (14), and (15). The critical properties used are those determined by the Bruce and Wilding finite-size scaling method, assuming Ising criticality—see Table I.

σ	$k_B T_c/\epsilon_{\text{eff}}$	$Z(\eta_c)$	$Z(\eta_c)/(k_B T_c/\epsilon_{\text{eff}})$
3	0.2986	0.3426	1.1473
1	0.3431	0.3707	1.0804
0.1	0.3694	0.3773	1.0213

V. DISCUSSION

In this paper we have used extensive MC simulations to investigate the liquid–vapor coexistence and the associated critical behavior in simple three-dimensional fluids with algebraic attractive interactions of varying range. We have studied three potentials, one of which is short-range ($\sim 1/r^6$), and is therefore expected to exhibit Ising criticality, and the other two are long-range ($\sim 1/r^4$, $\sim 1/r^{3.1}$), which have been predicted to exhibit classical critical behavior. With respect to the critical behavior, we have assumed the mixed-field ansatz, promoted by Bruce and Wilding, to make the link between fluid criticality and that of magnetic systems. In the absence of an accurate classical critical ordering operator distribution, $p_{\text{cl}}^{\star}(x)$, we have carried out the mixed-field finite-size scaling analyses using the universal Ising limiting distribution, $p_{\text{Is}}^{\star}(x)$. Deviations from Ising criticality then appear as inconsistencies in our analysis.

For the short-range potential the results are in accord with what one expects for a critical point which belongs to the three-dimensional Ising universality class. For the long-range potentials, however, the results show significant deviations from Ising criticality. In particular, it proved impossible to obtain an accurate collapse of the measured $p_L(x)$ onto $p_{\text{Is}}^{\star}(x)$. Moreover, the measured exponent ratio β/ν for both long-range potentials showed marked deviations from the established Ising value. On the other hand, it also proved impossible to fit $p_L(x)$ onto a theoretical estimate for $p_{\text{cl}}(x)$. This remains inconclusive until $p_{\text{cl}}(x)$ has been accurately measured in large-scale simulations of a suitably long-range model, such as the algebraic Ising model studied in Ref. 18.

We have obtained the infinite-volume critical parameters for each potential assuming Ising limiting forms, although those for the long-range potentials should only be considered as rough estimates. The values so obtained have been compared with a mean-field relation, due to Brilliantov and Valleau,[33] linking the critical temperature, the range of the potential, and the critical density, which is exact in the limit of an infinite-range potential. The simulation results suggest that the relation becomes increasingly accurate as the range of the potential increases, and hence that classical fluid criticality is approached in some fashion.

In summary, the long-range potentials simulated in this work show marked deviations from Ising criticality, assuming that the mixed-field ansatz in Eq. (2) is valid. In the light of recent work by Fisher and Orkoulas,[29,30] the prescription of the critical ordering operator, $\mathcal{M}$, employed in this work may not be complete. Fisher and Orkoulas suggest that the coexistence chemical potential is not analytic at the critical point, as there is some evidence of a diverging second temperature derivative, and that pressure terms may have to be included in the definition of $\mathcal{M}$. If this is indeed the case, the excellent agreement between the short-range $p_L(x)$ and $p_{\text{Is}}^{\star}(x)$ could be a result of the missing terms being small, for whatever reason.

This work obviously has implications for the study of fluid criticality in ionic systems, for which the universality class is uncertain. We have shown that there are subtle, but systematic, differences between $p_L(x)$ and $p_{\text{Is}}^{\star}(x)$ in long-range systems. In the case of the restricted primitive model, the reported $p_L(x)$ are of relatively poor quality compared to those measured in, say, Lennard-Jones fluids.[37] This is mainly due to the very low critical density in ionic fluids, which means that finite-size effects are pronounced even in large simulation boxes, particular in the vapor phase. Since $p_L(x)$ has not been measured very accurately in the RPM, it is quite difficult to assess the quality of the collapse onto the Ising limiting distribution.

It would be of interest to measure $p_{\text{cl}}^{\star}(x)$ in large-scale simulations of the long-range algebraic Ising model investigated in Ref. 18, which has already been shown to exhibit classical critical exponents. Once this distribution function is determined accurately, a more reliable finite-size scaling analysis could be carried out on fluids with long-range interactions to assess the consistency with classical criticality, assuming that the correct prescription of $\mathcal{M}$ is established.[29,30]

ACKNOWLEDGMENTS

We thank Dr. Nigel Wilding for supplying us with the ordering operator distribution function for the $D=3$ Ising model reported in Ref. 28. The financial support of the National Science and Engineering Research Council of Canada is gratefully acknowledged.

[1] S. Wiegand, M. E. Briggs, J. M. H. Levelt Sengers, M. Kleemeier, and W. Schröer, J. Chem. Phys. **109**, 9038 (1998).
[2] R. R. Singh and K. S. Pitzer, J. Chem. Phys. **92**, 6775 (1990).
[3] K. C. Zhang, M. E. Briggs, R. W. Gammon, and J. M. H. Levelt Sengers, J. Chem. Phys. **97**, 8692 (1992).
[4] T. Narayanan and K. S. Pitzer, J. Chem. Phys. **102**, 8118 (1995).
[5] J. M. Caillol and J.-J. Weis, J. Chem. Phys. **102**, 7610 (1995).
[6] P. J. Camp and G. N. Patey, Phys. Rev. E **60**, 1063 (1999).
[7] G. Stell, Phys. Rev. Lett. **32**, 286 (1974).
[8] J. M. Caillol, D. Levesque, and J. J. Weis, J. Chem. Phys. **107**, 1565 (1997).
[9] G. Orkoulas and A. Z. Panagiotopoulos, J. Chem. Phys. **110**, 1581 (1999).
[10] Q. Yan and J. J. de Pablo, J. Chem. Phys. **111**, 9509 (1999).
[11] G. Stell, Phys. Rev. B **1**, 2265 (1970).
[12] G. Stell, Phys. Rev. B **5**, 981 (1972).
[13] G. Stell, Phys. Rev. B **8**, 1271 (1973).
[14] M. E. Fisher, S. Ma, and B. G. Nickel, Phys. Rev. Lett. **29**, 917 (1972).
[15] J. Sak, Phys. Rev. B **8**, 281 (1973).
[16] R. Guida and J. Zinn-Justin, J. Phys. A **31**, 8103 (1998).
[17] M. Aizenman and R. Fernández, Lett. Math. Phys. **16**, 39 (1988).
[18] E. Luijten and H. W. J. Blöte, Phys. Rev. B **56**, 8945 (1997).
[19] H. W. J. Blöte, E. Luijten, and J. R. Heringa, J. Phys. A **28**, 6289 (1995).
[20] J. J. Rehr and N. D. Mermin, Phys. Rev. A **8**, 472 (1973).
[21] B. Widom, J. Chem. Phys. **43**, 3898 (1965).
[22] B. Widom and J. S. Rowlinson, J. Chem. Phys. **52**, 1670 (1970).
[23] N. D. Mermin, Phys. Rev. Lett. **26**, 169 (1971).
[24] N. D. Mermin, Phys. Rev. Lett. **26**, 957 (1971).

Downloaded 09 Aug 2013 to 129.215.221.120. This article is copyrighted as indicated in the abstract. Reuse of AIP content is subject to the terms at: http://jcp.aip.org/about/rights_and_permissions

[25] A. D. Bruce and N. B. Wilding, Phys. Rev. Lett. **68**, 193 (1992).
[26] N. B. Wilding and A. D. Bruce, J. Phys.: Condens. Matter **4**, 3087 (1992).
[27] D. Nicolaides and A. D. Bruce, J. Phys. A **21**, 233 (1988).
[28] R. Hilfer and N. B. Wilding, J. Phys. A **28**, L281 (1995).
[29] M. E. Fisher and G. Orkoulas, Phys. Rev. Lett. **85**, 696 (2000).
[30] G. Orkoulas, M. E. Fisher, and C. Üstün, J. Chem. Phys. **113**, 7530 (2000).
[31] R. Hilfer, Z. Phys. B: Condens. Matter **96**, 63 (1994).
[32] A. M. Ferrenberg and D. P. Landau, Phys. Rev. B **44**, 5081 (1991).
[33] N. V. Brilliantov and J. P. Valleau, J. Chem. Phys. **108**, 1123 (1998).
[34] N. Goldenfeld, *Lectures on Phase Transitions and the Renormalization Group*, 1st ed. (Addison-Wesley, New York, 1992).
[35] A. Z. Panagiotopoulos, Mol. Phys. **61**, 813 (1987).
[36] A. Z. Panagiotopoulos, N. Quirke, M. Stapleton, and D. Tildesley, Mol. Phys. **63**, 527 (1988).
[37] N. B. Wilding, Phys. Rev. E **52**, 602 (1995).
[38] F. J. Wegner, Phys. Rev. B **5**, 4529 (1972).
[39] J. H. Chen, M. E. Fisher, and B. G. Nickel, Phys. Rev. Lett. **48**, 630 (1982).
[40] M. P. Allen and D. J. Tildesley, *Computer Simulation of Liquids* (Clarendon, Oxford, 1987).
[41] B. Smit and D. Frenkel, Mol. Phys. **68**, 951 (1989).
[42] A. M. Ferrenberg and R. H. Swendsen, Phys. Rev. Lett. **61**, 2635 (1988).
[43] J. D. Weeks, D. Chandler, and H. C. Andersen, J. Chem. Phys. **54**, 5237 (1971).
[44] J. Hubbard and P. Schofield, Phys. Lett. **40A**, 245 (1972).
[45] E. Brézin and J. Zinn-Justin, Nucl. Phys. B **257 [FS14]**, 867 (1985).

Downloaded 09 Aug 2013 to 129.215.221.120. This article is copyrighted as indicated in the abstract. Reuse of AIP content is subject to the terms at: http://jcp.aip.org/about/rights_and_permissions